

High-order harmonic generation of Li^+ with combined infrared and extreme ultraviolet fields

Li Wang(王力), Guo-Li Wang(王国利)dag, Zhi-Hong Jiao(焦志宏), Song-Feng Zhao(赵松峰), Xiao-Xin Zhou(周效信)ddag
Citation: Chin. Phys. B . 2018, 27(7): 073205. **doi:** 10.1088/1674-1056/27/7/073205

Journal homepage: http://cpb.iphy.ac.cn; http://iopscience.iop.org/cpb

What follows is a list of articles you may be interested in

Modulation of multiphoton resonant high-order harmonic spectra driven by two frequency-comb fields

Yuanyuan Zhao(赵媛媛), Di Zhao(赵迪), Chen-Wei Jiang(蒋臣威), Fu-li Li(李福利)
Chin. Phys. B . 2018, 27(5): 053202. **doi:** 10.1088/1674-1056/27/5/053202

Isolated attosecond pulse generation with few-cycle two-color counter-rotating circularly polarized laser pulses

Jin-Song Wu(吴劲松), Zheng-Mao Jia(贾正茂), Zhi-Nan Zeng(曾志男)
Chin. Phys. B . 2017, 26(9): 093201. **doi:** 10.1088/1674-1056/26/9/093201

Restraint of spatial distribution in high-order harmonic generation from a model of hydrogen molecular ion

Chang-Long Xia(夏昌龙), Jun Zhang(张军), Xiang-Yang Miao(苗向阳), Xue-Shen Liu(刘学深)
Chin. Phys. B . 2017, 26(7): 073201. **doi:** 10.1088/1674-1056/26/7/073201

High-order harmonic generation of CO_2 with different vibrational modes in an intense laser field

Hui Du(杜慧), Hong-Dan Zhang(张宏丹), Jun Zhang(张军), Hai-Feng Liu(刘海凤), Xue-Fei Pan(潘雪飞), Jing Guo(郭静), Xue-Shen Liu(刘学深)
Chin. Phys. B . 2016, 25(11): 113201. **doi:** 10.1088/1674-1056/25/11/113201

Controlling the contributions to high-order harmonic generation from different nuclei of N_2 with an orthogonally polarizedtwo-color laser field

Hui Du(杜慧), Xue-Fei Pan(潘雪飞), Hai-Feng Liu(刘海凤), Hong-Dan Zhang(张宏丹), Jun Zhang(张军), Jing Guo(郭静), Xue-Shen Liu(刘学深)
Chin. Phys. B . 2016, 25(9): 093202. **doi:** 10.1088/1674-1056/25/9/093202

High-order harmonic generation of Li^+ with combined infrared and extreme ultraviolet fields*

Li Wang(王力), Guo-Li Wang(王国利)†, Zhi-Hong Jiao(焦志宏), Song-Feng Zhao(赵松峰), and Xiao-Xin Zhou(周效信)‡

Key Laboratory of Atomic and Molecular Physics and Materials of Gansu Province, College of Physics and Electronic Engineering, Northwest Normal University, Lanzhou 730070, *China*

(Received 30 January 2018; revised manuscript received 28 March 2018; published online 25 June 2018)

We investigate high-order harmonic generation (HHG) of Li^+ ion driven by an intense infrared (IR) laser field in combination with a weak XUV pulse. To achieve this, we first construct an accurate single-active electron angular-momentum-dependent model potential of Li^+ ion, by which the accurate singlet energy levels of Li^+ for the ground state and excited states with higher quantum numbers can be obtained. Then, we solve numerically the three dimensional time-dependent Schrödinger equation of Li^+ ion by means of the generalized pseudospectral method to obtain HHG. Our results show that the strength of assisted XUV is not amplified during the harmonic generation process, but the yield of HHG power spectrum in the whole plateau has a significant enhancement. Furthermore, the optimal phase delay between the IR and XUV pulses allows the production of ultrabroadband supercontinuum spectra. By superposing some harmonics, a strong new single 27-attosecond ultrashort pulse can be obtained.

Keywords: high-order harmonic generation, model potential of Li^+, enhancement, attosecond pulse

PACS: 32.80.Rm, 42.65.–k, 42.65.Ky **DOI:** 10.1088/1674-1056/27/7/073205

1. Introduction

Laser-driven high-order harmonic generation (HHG) has received continuous research interest in the past thirty years after its first observations at the end of 1980's.[1,2] As a promising tabletop source of broadband extreme-ultraviolet (XUV) light with excellent spatial and temporal coherence, HHG has been used for x-ray coherent diffractive imaging,[3] solid spectroscopy,[4,5] etc. The HHG is also a reliable route to produce short attosecond light pulses and is therefore fundamental to attosecond science.[6–11] At present, however, the efficiency of conversion to high-order harmonics is really so small that it hinders the applications of HHG. Hence, the search for ways of increasing the HHG efficiency in the XUV spectral range is still among the most pressing problems of strong field physics. In general, in terms of the incident laser pulse, the techniques of femtosecond temporal and spatial laser pulse shaping (see Refs. [12] and [13] and references therein) the waveform synthesizing with multi-color laser fields[14] can be used to achieve this to some extent.

Recently, a strong-field-mediated intrapulse x-ray parametric amplification (IXPA) process has been claimed by Serrat *et al.*[15–18] In this process, a weak XUV pulse can be largely enhanced when it is optimally synchronized with the intense IR pulse to generate HHG. In the optimal parameter ranges, this effect can result in exponential growth of the XUV–x-ray signal in tabletop XUV–x-ray lasers. Such a mechanism is worth the verification by more careful simulations due to its attractive application.[19]

Due to the high ionization potential, Li^+ was considered an ideal amplifying medium to demonstrate the IXPA effect by solving the one-dimensional (1D) time-dependent Schrödinger equation (TDSE) in Ref. [18]. In the 1D-TDSE simulations, the contribution from excited states and the effect of spreading of the electron wavepacket on HHG are not given careful consideration. In the present paper, we reinvestigate this issue. We will first construct an accurate angular-momentum-dependent model potential for Li^+ ion to replace the soft-Coulomb potential used in Ref. [18]. Then we calculate harmonic spectra by solving a three-dimensional (3D) time-dependent Schrödinger equation (TDSE), and tell the difference between present simulations and 1D TDSE results shown in Ref. [18] . The present paper is organized as follows: in Section 2, we introduce briefly the theoretical methods. In Section 3, we present our simulated results and discussions. Then we end with a conclusion in Section 4. Atomic units (a.u.) are used throughout this paper unless otherwise indicated.

2. The simulation method

To get the HHG of Li^+ ion in the laser field, we solve the following 3D TDSE:

$$\mathrm{i}\frac{\partial}{\partial t}\psi(\boldsymbol{r},t) = \hat{H}(\boldsymbol{r},t)\psi(\boldsymbol{r},t), \tag{1}$$

*Project supported by the National Natural Science Foundation of China (Grant Nos. 11465016, 11664035, 11764038, and 11765018) and the Foundation of Northwest Normal University, China (Grant No. NWNU-LKQN-17-1).

†Corresponding author. E-mail: wanggl@nwnu.edu.cn

‡Corresponding author. E-mail: zhouxx@nwnu.edu.cn

© 2018 Chinese Physical Society and IOP Publishing Ltd

where Hamiltonian $\hat{H}(r,t)$ can be separated into two terms as

$$\hat{H}(\boldsymbol{r},t) = H_0(\boldsymbol{r}) - \boldsymbol{E}(t)\cdot\boldsymbol{r}. \tag{2}$$

Here, $-\boldsymbol{E}(t)\cdot\boldsymbol{r}$ represents the time-dependent interaction of Li^+ and laser field, $H_0(\boldsymbol{r})$ is the field-free Hamiltonian of Li^+ ion which has the form

$$H_0(\boldsymbol{r}) = -\frac{1}{2}\nabla^2 + \sum_l |Y_l^0\rangle V_l \langle Y_l^0|, \tag{3}$$

where Y_l^0 is the spherical harmonic. To obtain accurate harmonic spectra, an angular-momentum-dependent model potential V_l has been proposed for He in Ref. [20] , which will also be adopted in the present simulation, but the values of parameters in V_l need to be redetermined. Such a potential has the form as

$$V_l(r) = -\frac{\alpha_p}{2r^4}W_6\left(\frac{r}{r_c}\right) - \frac{2}{r} - \left(\frac{N-S}{r} + A_1\right)e^{-B_1 r} - \left(\frac{S}{r} + A_2\right)e^{-B_2 r}. \tag{4}$$

The total number of l used in the present simulations is 80. In the formula above, α_p is the core dipole polarizability of Li^{2+},[21] r_c is an effective Li^{2+} core radius, and W_6 is a core cutoff function given by

$$W_n(x) = 1 - \left[1 + nx + \frac{(nx)^2}{2!} + \frac{(nx)^3}{3!} + \cdots + \frac{(nx)^n}{n!}\right]e^{-nx}. \tag{5}$$

For the given potential V_l and electric field $E(t)$ of the laser pulse, equation (1) is numerically solved in space and time with the time-dependent generalized pseudospectral method (TDGPS).[22] In this technique, the spatial coordinates are nonuniform grids: the denser points near the core and sparser points for the larger distances. For the time propagation of the wave function, a second-order split-operator technique in the energy representation is adopted which allows the explicit elimination of undesirable fast-oscillating high-energy components:

$$\psi(t+\Delta t) = e^{-iH_0\Delta t/2}e^{[i\boldsymbol{E}(t+\Delta t/2)\cdot\boldsymbol{r}\Delta t]}e^{-iH_0\Delta t/2}\psi(t) + o\left(\Delta t^3\right). \tag{6}$$

The detailed numerical method of solving Eq. (6) can be found in Ref. [22]. Once the time-dependent wave function is obtained, we can get the lengthform induced dipole momentum

$$d_L(t) = \langle\psi(\boldsymbol{r},t)|z|\psi(\boldsymbol{r},t)\rangle, \tag{7}$$

where z is the distance between the electron and the core along the polarization direction of the linearly polarized laser field.

Then the HHG power spectrum can be obtained by Fourier transformation of induced dipole momentum $d_L(t)$,

$$d_L(\omega) = \left|\frac{1}{t_f - t_i}\int_{t_i}^{t_f} d_L(t)\, e^{-i\omega t}\,dt\right|^2. \tag{8}$$

Attosecond pulse can be produced by superposing some harmonics

$$I(t) = \left|\sum_n e^{in\omega t}\int d(t)e^{-in\omega t'}\,dt'\right|^2. \tag{9}$$

To obtain the temporal and spectral characteristics of the harmonics, we perform the time-frequency analysis[23,24] in terms of the wavelet transform of the induced dipole

$$A(t_0,\omega) = \int d(t)\sqrt{\omega}W[\omega(t-t_0)]\,dt \tag{10}$$

with the Morlet wavelet

$$W(x) = \frac{1}{\sqrt{\tau}}e^{ix}e^{-\frac{x^2}{2\tau^2}}. \tag{11}$$

3. Results and discussion

3.1. The parameters for the model potential of Li^+

To take the influence of accurate atomic structure on the harmonic spectra into account, we first fit the parameters for the model potential given in Eq. (2), by comparing the singlet energy levels calculated from solving the stationary state Schrödinger equation and standard values from NIST.[25] The determined parameter values for four different angular momenta are given in Table 1.

Table 1. Model potential parameters for Li^+ (in atomic units).

l	α	r_c	S	A_1	A_2	B_1	B_2
0	0.055528	1.95	–1.8372	–63.85	91.10002	3.45	4.9
1	0.055528	1.95	–0.0294	–0.847	0.00144	1.74	0.0
2	0.055528	1.95	0.0	0.0	0.0	4.3	0.0
$\geqslant 3$	0.055528	1.95	0.0	0.0	0.0	3.8	0.0

Table 2. Comparison between present calculated singlet energy levels and standard values from NIST[25] (in atomic units).

n \ l	0		1		2		3	
	present	NIST[25]	present	NIST[25]	present	NIST[25]	present	NIST[25]
1	–2.779722	–2.779722						
2	–0.540851	–0.540854	–0.493312	–0.493314				
3	–0.233758	–0.233743	–0.220181	–0.220188	–0.222373	–0.222371		
4	–0.129774	–0.129772	–0.124156	–0.124153	–0.125066	–0.125060	–0.125015	–0.125001
5	–0.082421	–0.082419	–0.079824	–0.079479	–0.080035	–0.080027	–0.080009	–0.079998
6	–0.056949	–0.056945	–0.055796	–0.055781	–0.055577	–0.055569	–0.055562	–0.055551
7	–0.041691	–0.041684	–0.041334	–0.041374	–0.040831	–0.040822	–0.040821	–0.040811

To assess the accuracy of this model potential, we compare the calculated energy levels with those from NIST[25] in Table 2. It is shown that the two set energies are in good agreement with each other, for both ground state and excited states up to $n = 7$, $l = 3$, where n and l are the principle and orbital quantum number, respectively. So our model potential would be safely used to simulate the HHG.

3.2. HHG of Li^+ in the combined laser field

Figure 1 presents our simulated HHG spectra of Li^+ generated by single-color 800-nm IR laser field and combined two-color field consisting of IR and a weak XUV pulses. The parameters used in the calculations are $r_{max} = 150$ a.u. with $N = 1500$ radial grid points. The IR and XUV pulses are identical with those used in Ref. [18]. The IR laser intensity is 2.5×10^{15} W/cm^2 in all the case, and the total pulse duration is 4 optical cycles with a sin^2 envelope. The central wavelength of XUV is 10.97 nm (which corresponds to the 73rd harmonic of IR laser), and the duration is chosen as 200 attoseconds with the same pulse shape as IR laser. The calculated harmonic cutoff energy is about 387 eV (the 250th harmonic of fundamental laser pulse), which agrees with both the classical calculation by solving the Newton equation and 1D-TDSE simulation,[18] but it deviates from the commonly used law of $I_p + 3.17U_p$ due to the very short pulse used, where I_p is the ionization potential of the ground state of Li^+, U_p is the ponderomotive energy of returning electrons. However, as expected, the detailed spectral structures between present simulations and those from 1D-TDSE simulation[18] are not totally the same. Usually, the excited states may play roles in the HHG.[26,27] Nevertheless, in our case the populations of excited states are very small. The main contribution from excited states is that the energy difference between the ground state and first excited state (2p) results in a broad structure around the 40th harmonic. We note that present simulations are carried out on the basis of the single-active electron (SAE) approximation. Compared with the SAE calculations, the correlation effect of electrons in the time-dependent field can change the harmonic strength, cutoff energy, and result in a new broader structure in the higher energy region due to resonance between the intermediate state and the ground state.[28,29] Since we compare only the relative HHG spectra, our conclusion given below will remain even after considering the correlation effect.

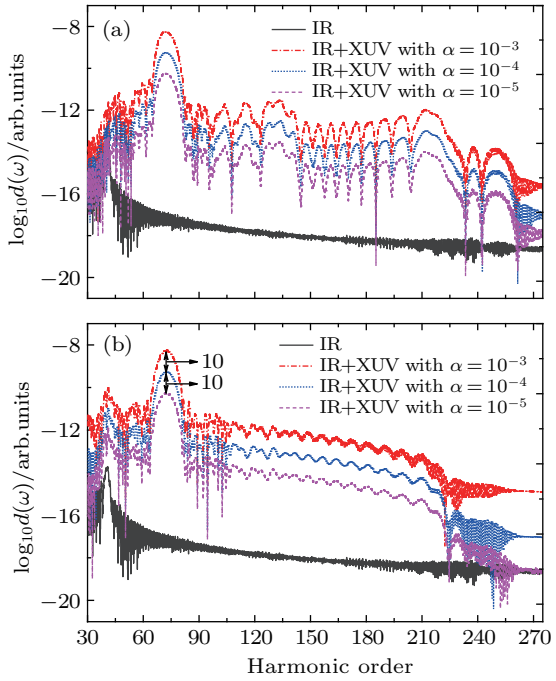


Fig. 1. HHG spectra of Li^+ generated by single 800-nm IR laser and two-color IR+XUV pulse for two phase delays of (a) 0° and (b) 75°. The peak intensity of IR is 2.5×10^{15} W/cm^2 in all cases, while XUV intensity is determined by three α values of 10^{-3}, 10^{-4}, and 10^{-5}. Here, $\alpha = I_{XUV}/I_{IR}$ is the ratio between XUV and IR peak intensities. The central wavelength of XUV pulse corresponds to the 73th harmonic of the fundamental 800 nm wavelength.

The first issue we want to confirm is whether the XUV pulse is amplified during the HHG. To do this we simulate harmonic spectra with three different XUV intensities of 2.5×10^{10} W/cm^2, 2.5×10^{11} W/cm^2, and 2.5×10^{12} W/cm^2 (in the simulation of Serrat *et al.*,[18] only one XUV intensity is considered), for two relative phase delays of 0° and 75° with respect to the IR pulse, respectively. By comparing the three harmonic spectra generated with XUV assisted two-color fields, from Figs. 1(a) and 1(b) we can see that for two delays the same enhancement of 10 is obtained for the 73rd harmonic for all XUV intensities, which is just the ratio between the three XUV intensities from high to low. In addition, in the same way as that used in Ref. [19] , we also compare the harmonic spectra with incident XUV pulses directly. We find they overlap one another for two delays (not shown here). Thus, unlike the statement shown in Ref. [18] that was based on the 1D-TDSE simulation, in present simulations we do not see the obvious XUV amplification, similar to the one pointed out in Ref. [19] for the medium of He. Simulations with more delays also show no sensitive timing dependence for the strength of the 73rd harmonic.

The other striking feature shown in Fig. 1 is the large enhancement of harmonics over the whole spectral plateau with the assistance of a weak XUV pulse, which has also been observed in the 1D TDSE simulations.[18] Such an increase would be very important for the HHG application. With an intensity of 2.5×10^{10} W/cm^2, which corresponds to a ratio of only 10^{-5} between XUV and IR fields, the presence of XUV makes harmonics generated by IR alone simultaneously enhanced by about four orders of magnitude. It is also shown that the harmonic yield varies only linearly with the XUV intensity. Figure 2 shows the ionization probabilities of Li^+ in different laser fields. It shows that the enhancement factor of ionization probabilities of Li^+ in the various laser fields also depends linearly on the XUV intensity. These behaviors have been observed in the case of the long IR and attosecond pulse

train (APT) earlier,[30] and can be understood as a result of two effects from the view of a semiclassical model of harmonic generation processes. First, the ionization of electron from the initial ground state to continuum is a one-photon process for the XUV pulse, and hence has a large probability compared to the case of IR laser. Second, the most electrons released within a proper narrow time interval via one-photon ionization are likely to return to the core, compared to when they are released throughout the whole cycle as in tunneling ionization for IR. Under this assumption, the harmonic yield can be more effectively enhanced using XUV-assisted field, even with the comparable ionization level compared to the IR field (see the black and magenta lines shown in Figs. 1 and 2). It is worth noting that such enhancement has been confirmed by macroscopic simulations.[30]

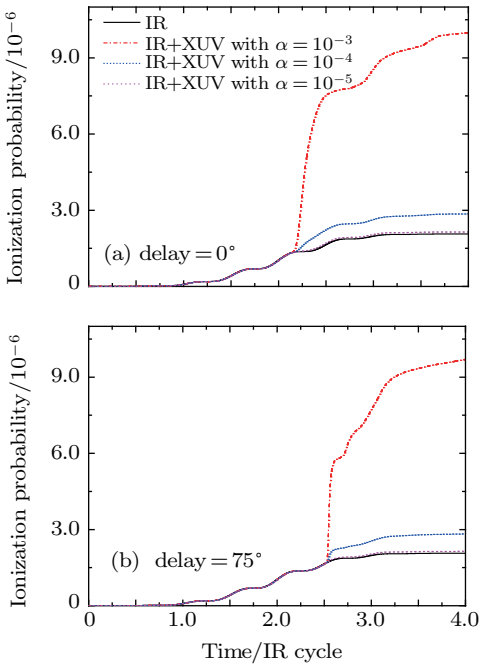


Fig. 2. (color online) Ionization level of Li^+ in the IR and IR + XUV laser fields for the parameters used in Fig. 1.

We also simulate HHG generated by a new assisted XUV with the photon energy of 15.946 a.u. (corresponding to the 280th harmonic of IR), which is bigger than the harmonic cutoff generated by IR laser alone. The simulated spectrum is shown in Fig. 3. For reference, the harmonic spectrum generated by the IR pulse alone is also shown. From the comparison, we can see that in this case, the IR+XUV generated harmonics overlap the IR generated spectrum below the cutoff, except for the strong response at the XUV harmonic, that is, there is no XUV induced harmonic amplification at all. We perform the calculation of classical electron dynamics in the combined IR + XUV electric field. Because ionization proceeds mainly via one-photon absorption, the electron is released with a nonzero kinetic energy as $E_k = h\nu - I_p - U_p$. Under this assumption, the electron fails to return to the ion core to give rise to the harmonic generation.

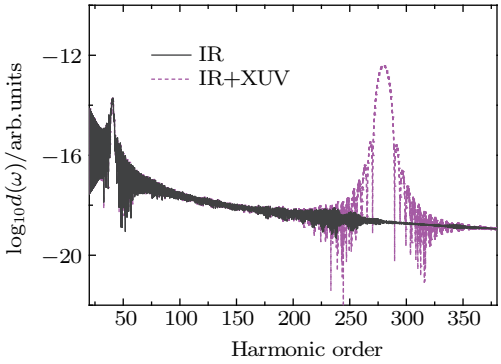


Fig. 3. (color online) Same as Fig. 1(a), but for the XUV central wavelength of the 280th harmonic of IR. The peak intensity of IR and XUV pulses are 2.5×10^{15} W/cm^2 and 2.5×10^{10} W/cm^2, respectively.

3.3. New single ultrashort pulse generation

Another apparent role of the XUV pulse is quantum path selection. A similar application has been found for APT.[31] The harmonics in IR generated spectrum is unresolved because of chirp-induced spectral broadening.[30] The resolution of harmonics in the two-color field is greatly improved, which indicates the XUV pulse can select particular quantum paths. Furthermore, it is obvious that such selection is sensitive to the phase delay between IR and XUV pulse. Although the harmonic yields for the two-color laser fields shown in Figs. 1(a) and 1(b) are almost the same, the spectral structures are apparently different. For the delay of 0°, harmonic spectra contain the strong oscillations. Adding a weak XUV pulse with a delay of 75° with respect to the IR laser can smooth the harmonic spectra effectively. To understand the physical mechanism for these differences, take XUV intensity of 2.5×10^{11} W/cm^2 for example, we perform the quantum time-frequency analysis for the harmonics generated by two-color fields, which is shown in Fig. 4. We can see that the harmonic emission above about 120 eV is different for two phase delays. In the case of 0°, there are two main emissions. While for the delay of 75°, the adding of XUV pulse suppresses one trajectory. Hence,

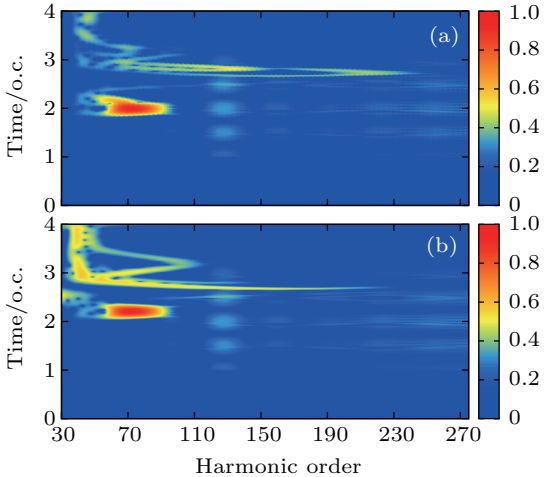


Fig. 4. Wavelet time-frequency profiles of harmonics generated by two-color laser fields with XUV intensity of 2.5×10^{11} W/cm^2 for two delays of (a) 0° and (b) 75°, respectively.

the absence of interference makes the harmonic spectrum continuous. In this case, by superposing harmonics from 110th to 215th, as shown in Fig. 5, a single attosecond pulse with duration as short as 27 attosecond can be generated.

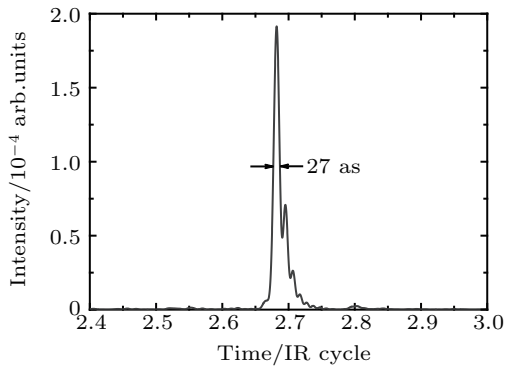


Fig. 5. The temporal profile of the single attosecond pulse generated by superposing directly from 110th to 215th harmonics shown in Fig. 1(b) with the blue line.

4. Conclusions

The generation of intense high-order harmonics and single attosecond pulses has crucial importance for their applications. For this purpose, in this work, we investigate the response of Li^+ with a short IR laser field in combination with a weak XUV pulse. One of our important contributions is that we construct an accurate model potential for Li^+, by which we can study not only the HHG from the ground and low excited states of Li^+, but also the properties of excitation in the laser field. Unlike the previous 1D-TDSE results where we observe the strong-field-driven x-ray parametric amplification, our 3D-TDSE simulations show that the strength of assisted XUV pulse is not amplified during the harmonic generation process. However, the harmonic yield is enhanced dramatically due to the large ionization level and the probability of electrons backing to the core induced by one-photon absorption of XUV pulse. Furthermore, the proper adding of XUV makes the harmonic spectrum continuous, and a strong single attosecond pulse with new central frequency and shorter width can be generated.

References

[1] McPherson A, Gibson G, Jara H, Johann U, Luk T S, McIntyre I, Boyer K and Rhodes C K 1987 *J. Opt. Soc. Am. B* **4** 595
[2] Ferray M, Huillier A l, Li X, Lompre L, Mainfray G and Manus C 1988 *J. Phys. B: At. Mol. Opt. Phys.* **21** L31
[3] Miao J, Ishikawa T, Robinson I K and Murnane M M 2015 *Science* **348** 530
[4] Vampa G, Hammond T J, Thiré N, Schmidt B E, Légaré F, McDonald C R, Brabec T, Klug D D and Corkum P B 2015 *Phys. Rev. Lett.* **115** 193603
[5] Luu T T, Garg M, Yu S, Moulet A, Th M and Goulielmakis E 2015 *Nature* **521** 498
[6] Chang Z, Corkum P B and Leone S R 2016 *J. Opt. Soc. Am. B: Opt.* **33** 1081
[7] Calegari F, Sansone G, Stagira S, Vozzi C and Nisoli M 2016 *J. Phys. B: At. Mol. Opt. Phys.* **49** 062001
[8] Krausz F 2016 *Phys. Scr.* **91** 063011
[9] Wu J S, Jia Z M and Zeng Z N 2017 *Chin. Phys. B* **26** 093201
[10] Li F, Wang G L, Zhao S F and Zhou X X 2015 *Chin. Phys. Lett.* **32** 014210
[11] Qin Y F, Guo F M, Li S Y, Yang Y J and Chen G 2014 *Chin. Phys. B* **23** 0104211
[12] Winterfeldt C, Spielmann C and Gerber G 2008 *Rev. Mod. Phys.* **80** 117
[13] Wang G L, Li P C, Li X Y, Zhao S F and Zhou X X 2017 *Sci. China-Phys. Mech. Astron.* **47** 033002 (in Chinese)
[14] Jin C, Wang G, Wei H, Le A T and Lin C D 2014 *Nat. Commun.* **5** 4003
[15] Serrat C 2013 *Phys. Rev. Lett.* **111** 133902
[16] Serrat C, Roca D and Seres J 2015 *Opt. Express* **23** 4867
[17] Serrat C, Roca D, Budesca J M, Seres J, Seres E, Aurand B, Hoffmann A, Namba S, Kuehl T and Spielmann C 2016 *Opt. Express* **24** 8028
[18] Serrat C 2016 *Phys. Rev. A* **93** 063415
[19] Bredtmann T, Patchkovskii S and Ivanov M 2016 *Phys. Rev. Lett.* **117** 109401
[20] Li P C, Laughlin C and Chu S I 2014 *Phys. Rev. A* **89** 023431
[21] Szmytkowski R and Łukasik G 2016 *At. Data Nucl. Data Tables* **111** 41
[22] Tong X M and Chu S I 1997 *Chem. Phys.* **217** 119
[23] Tong X M and Chu S I 2000 *Phys. Rev. A* **61** 021802
[24] Chui C K 1992 *An Introduction to Wavelets* (New York: Academic Press)
[25] *NIST Atomic Spectra Database* (ver. 5.5.1) http://physics.nist.gov/asd
[26] Bian X B and Bandrauk A D 2010 *Phys. Rev. Lett.* **105** 093903
[27] Beaulieu S, Camp S, Descamps D, Comby A, Wanie V, Petit S, Légaré F, Schafer K J, Gaarde M B, Catoire F and Mairesse Y 2016 *Phys. Rev. Lett.* **117** 203001
[28] Hu S L and Shi T Y 2013 *Chin. Phys. B* **22** 013101
[29] Guan X, Tong X M and Chu S I 2006 *Phys. Rev. A* **73** 023403
[30] Gaarde M B, Schafer K J, Heinrich A, Biegert J and Keller U 2005 *Phys. Rev. A* **72** 013411
[31] Schafer K J, Gaarde M B, Heinrich A, Biegert J and Keller U 2004 *Phys. Rev. Lett.* **92** 023003